

On the displacement of fluid bridges from solid surfaces in viscous pressure-driven flows

P. Dimitrakopoulos

Department of Chemical Engineering, University of Maryland, College Park, Maryland 20742

J. J. L. Higdon

Department of Chemical Engineering, University of Illinois, Urbana, Illinois 61801

(Received 4 February 2003; accepted 22 July 2003; published 5 September 2003)

The yield conditions for the displacement of three-dimensional fluid bridges from solid boundaries are studied in pressure-driven Stokes flows. The study seeks the optimal shape of the contact line that yields the maximum flow rate for which a fluid bridge can adhere to the surfaces. The contact line contours show fore-and-aft asymmetry with a distorted shape not well represented by simple circular/elliptical planforms. The critical shear rate is shown to be sensitive to viscosity ratio; as the viscosity of the bridge increases, the critical shear rate decreases facilitating the displacement. The effects of the contact angles are found to be similar for both viscous and inviscid bridges, in direct contrast with our earlier results for drop displacement from a single substrate. The critical flow rate is strongly affected by the plate spacing; bridges with moderate height are shown to withstand the highest flow rate. This behavior is readily explained employing scaling analysis. © 2003 American Institute of Physics. [DOI: 10.1063/1.1609443]

In this article we consider the yield criteria for displacement of three-dimensional fluid bridges spanning the gap between two parallel plates in pressure-driven flows. Our interest focuses on bridge displacement in viscous flows at low-Reynolds number. This regime has relevance in the operation of coating machines and other devices (e.g., microfluidics) involving flow between closely spaced parallel plates. The fundamental issues associated with viscous drop displacement from rigid boundaries have been addressed by Dussan based on asymptotic theory valid for small contact angles,¹ and in our previous work²⁻⁴ where we addressed the drop displacement problem making no restrictions on the problem parameters. Further references on droplet displacement and contact angles may be found in our earlier papers.²⁻⁴

In the present study, we turn our attention to the displacement of fluid bridges. To this date there has been no study which considers the displacement of a general three-dimensional fluid bridge between two parallel plates in pressure-driven flows. Due to the existence of the (continuous) contact line for the three-dimensional problem, for a given material system (i.e., bridge and surrounding fluids, and solid surfaces) there exist many different bridge configurations. In our study, we seek the optimal shape of the contact line which provides the maximum flow rate (or capillary number Ca) for which a bridge can adhere to the solid surfaces. For a given material system, the maximum flow rate Ca represents the yield condition for displacement in the sense that a higher flow rate will always displace the bridge. (On the other hand, a specific fluid bridge may be displaced under a smaller flow rate if the bridge is unable to achieve its optimal shape.)

Under this flow condition, both the shape of the contact

line and the bridge interface are *equilibrium* shapes, independent of the hydrostatic shape of the bridge and the conditions of the transient deformation. While we compute these equilibrium shapes under different flow conditions, we do not attempt a stability analysis for these complicated three-dimensional shapes. Such an analysis represents a challenging problem beyond the scope of the present effort.

We consider a fluid bridge between two parallel plates; the bridge size is specified by the radius a of a spherical droplet of the same volume, while the surface tension γ is assumed to be constant. The undisturbed flow exterior to the bridge is a plane Poiseuille flow at low-Reynolds-number while gravitational effects are excluded by restricting our analysis to bridges for which a characteristic Bond number is negligible. We assume the bridges are symmetric about the midplane, but allow fore-aft asymmetry associated with deformation in the flow direction x . Note that the (midplane) z symmetry is a requirement for stability of axisymmetric bridges in quiescent conditions.⁵ For a stationary contact line, the contact angle θ should always be $\theta_A \leq \theta \leq \theta_R$, where θ_A and θ_R are the advancing and receding angles, respectively. The relevant parameters of the current problem include the capillary number $Ca \equiv \mu G a / \gamma$ (where G is the velocity gradient at the lower wall), the ratio λ of the bridge viscosity to that of the surrounding fluid (μ), the angles θ_A and θ_R (or equivalently θ_A and the hysteresis $\theta_A - \theta_R$) as well as the dimensionless distance between the two plates H/a . The computational procedure consists of an efficient three-dimensional Newton method to determine the equilibrium shape of fluid interfaces, combined with an optimization algorithm to solve for the optimal shape of the contact line, as presented in our recent paper on drop displacement in shear flows.²

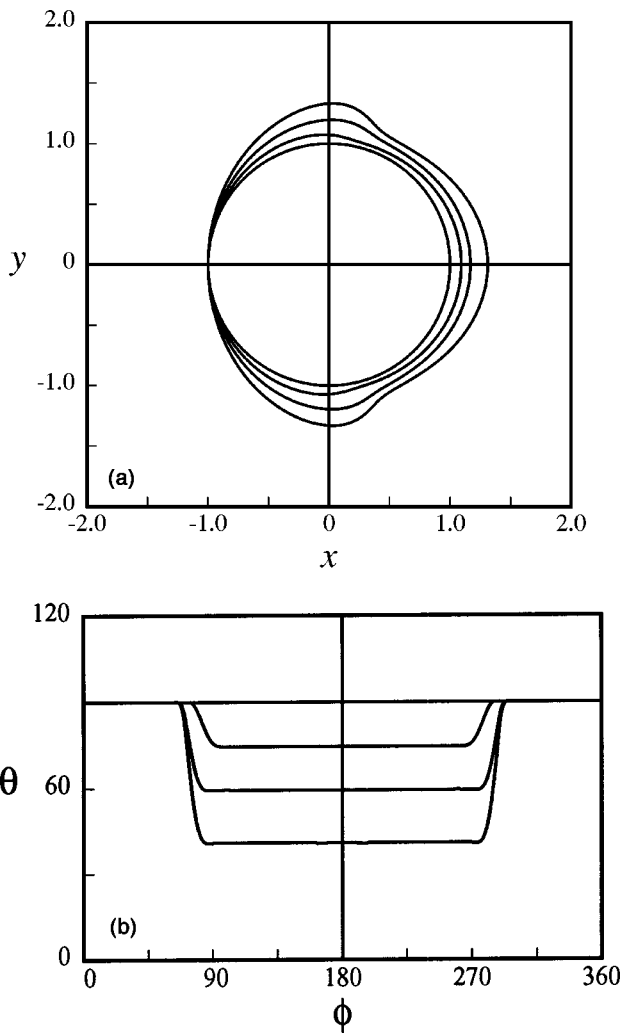


FIG. 1. Equilibrium shapes for bridges with $\lambda = 1$ and $\theta_A = 90^\circ$, for $H/a = 1.747$ and $Ca = 0, 0.05, 0.10, 0.155$. (a) The optimal shape of the contact line. (b) The variation of the contact angle θ as a function of the azimuthal angle ϕ measured with respect to the positive x direction.

We begin our investigation by considering the displacement of a liquid bridge with $\lambda = 1$. Figure 1 shows the contact line contours and the distribution of contact angles around the contact line for a bridge with $\theta_A = 90^\circ$, for $H/a = 1.747$ and several values of the capillary number Ca . (This value of H/a corresponds to a cylindrical bridge with height twice its radius.) This figure shows the two common features of the optimal contact lines;^{2,4} as the flow rate is increased both the length and the width of the contact line increase. As explained in our previous studies, the increased hysteresis and contact line width both act to increase the interfacial force necessary to balance the higher hydrodynamic forces on the bridge. In addition, the downstream portion of the contact line admits a single maximum angle θ_A while its upstream portion admits a single minimum angle θ_R , while between the two portions there is an acute jump in the distribution of the contact angles. This distribution is a further consequence of the bridge's attempts to maximize the interfacial force: the bridge holds the minimum angle over the entire front of the contact line, then makes the fastest possible transition to the maximum angle on the rear-facing con-

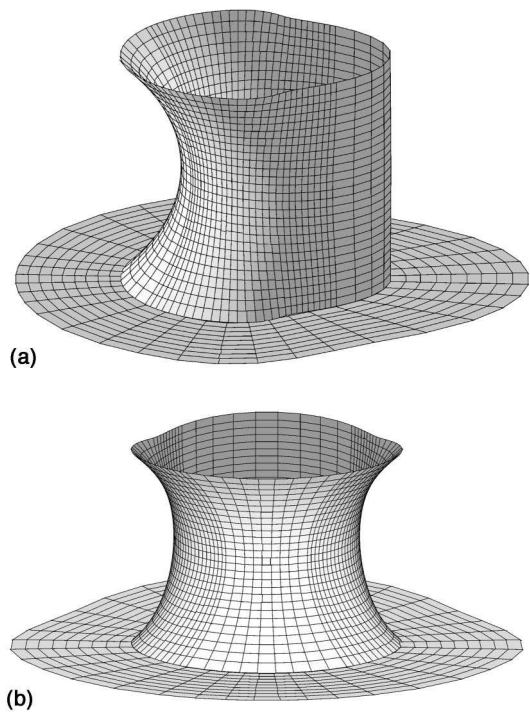


FIG. 2. Bridge surface for $\lambda = 1$, $\theta_A = 90^\circ$, and $Ca = 0.155$.

tour. The resulting highly asymmetric bridge shape is shown in Fig. 2 for a specific flow rate Ca .

Figure 3 shows the critical Ca as a function of hysteresis $\theta_A - \theta_R$, for $H/a = 1.747$ and several values of θ_A . For a given hysteresis, increasing the contact angle θ_A from small values, *increases* the critical flow rate, for values of the advancing angle up to $\theta_A \approx 90^\circ$. Above this value, increasing the contact angle θ_A *decreases* the critical flow rate. Thus the influence of the advancing angle θ_A on the displacement of a viscous bridge is qualitatively similar to that for a viscous

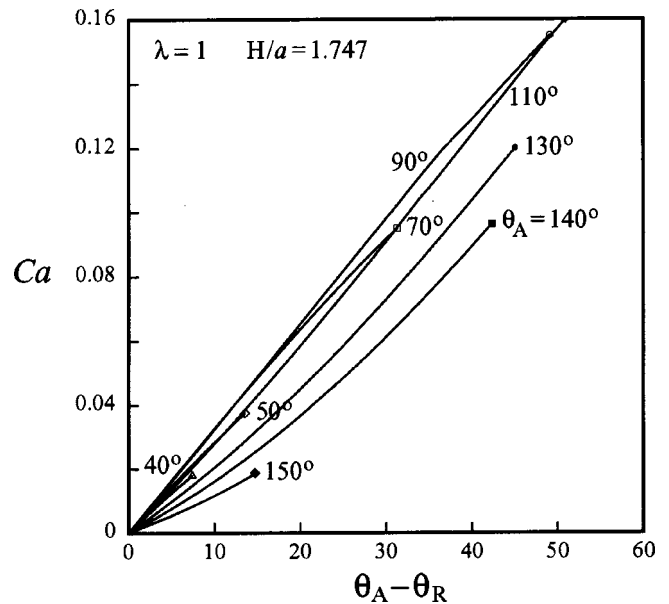


FIG. 3. Critical capillary number Ca vs hysteresis $\theta_A - \theta_R$ for a viscous bridge.

droplet in shear and pressure-driven flows^{2,4} as well as to that on the gravitational displacement of fluid droplets.³ This behavior is associated with changes in the net interfacial force. For small hysteresis, this force is proportional to the width of the droplet (or radius of the contact line) and the quantity $(\cos \theta_R - \cos \theta_A)$ which measures the component of the force parallel to the wall. The radius of the contact line decreases monotonically with θ_A , while the quantity $(\cos \theta_R - \cos \theta_A)$ scales as $(\theta_A - \theta_R) \sin \theta_A$ for small hysteresis. It increases for small θ_A but reaches a maximum at $\theta_A = 90^\circ$. Increasing θ_A from small values, the radius of the contact line decreases, while $\sin \theta_A$ increases toward its maximum value. The net interfacial force increases, and hence a stronger flow rate Ca is required to displace the bridge. At angles slightly below $\theta_A = 90^\circ$, the effect of the reducing radius becomes dominant, and the interfacial force begins to decrease. For angles above $\theta_A = 90^\circ$, both the radius and the $\sin \theta_A$ term decrease as θ_A increases; thus the critical Ca decreases facilitating the displacement.

This behavior is valid for small and moderate values of hysteresis, as clearly shown in Fig. 3 above. A careful examination of this figure shows that the curves for bridges with $\theta_A \leq 90^\circ$ (usually called wetting bridges in hydrostatic problems) exhibit a different slope compared to the ones for bridges with $\theta_A > 90^\circ$ (or non-wetting bridges in hydrostatic problems). By extrapolating our numerical results to high hysteresis, e.g., $\theta_A - \theta_R \rightarrow \theta_A$, one may speculate that bridges with $\theta_A > 90^\circ$ might become more stable than bridges with $\theta_A = 90^\circ$ at high enough values of hysteresis. This conclusion is in agreement with the behavior at high hysteresis of the curves for $\theta_A = 90^\circ$ and $\theta_A = 110^\circ$ shown in Fig. 3.

Investigating the effects of the viscosity ratio λ , we found that the influence of θ_A on inviscid or low-viscosity bridges ($\lambda \leq 1$) as well as on high-viscosity bridges ($\lambda \gg 1$) is qualitatively similar to that for $\lambda = 1$ at any plate spacing, i.e., for both short and tall bridges. For inviscid bridges at large plate spacings, the dominant displacing force is the pressure force associated with the disturbance of the base flow. On the other hand, for small plate spacings the dominant pressure force is associated with the pressure gradient. Thus for fluid bridges the two pressure components and the shear stress show similar dependence on the advancing angle θ_A . This behavior differs from our earlier results for a drop attached to a single wall in parabolic flow between two plates. For small plate spacing, viscous and inviscid droplets show similar behavior consistent with the present results. However, for large plate spacing the influence of θ_A on an inviscid droplet is diametrically opposite to that for a viscous droplet.⁴ The explanation for this behavior lies on the force balance on the bridge. For both viscous and inviscid bridges, the pressure force is proportional to the frontal area of the bridge. For viscous bridges there is an additional force, the shear stress, which is proportional to the surface area of the bridge. For a bridge spanning the gap between two parallel walls, the frontal and surface areas are comparable; thus both viscous and inviscid bridges are affected similarly by the advancing contact angle θ_A . Owing to the shear stress, the viscous bridges require more hysteresis and exhibit more de-

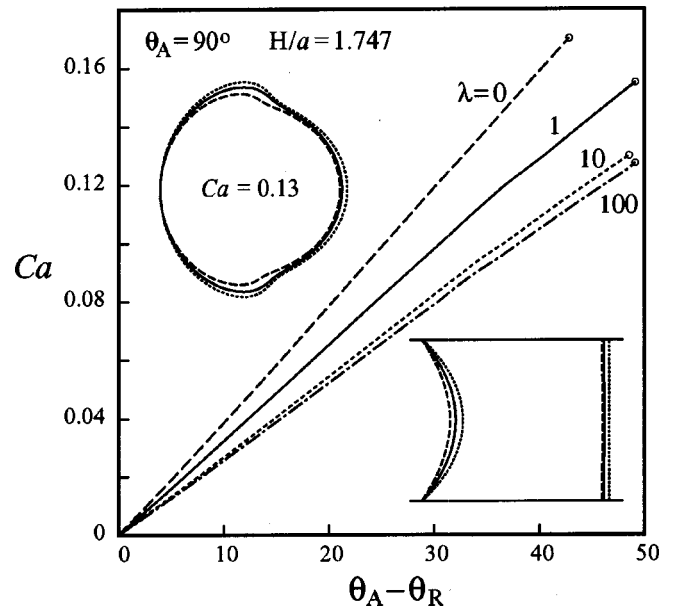


FIG. 4. Critical Ca vs hysteresis $\theta_A - \theta_R$ for several viscosity ratios. Also shown are the contact line shapes and bridge profiles for $Ca = 0.13$.

formation as shown in Fig. 4 below (where we collect results for several viscosity ratios). However, this effect is not as strong for bridges as it is for droplets. The droplets may become quite spread out over the surface reducing the pressure force and thus resulting in large deviations for the critical flow rate Ca as the viscosity ratio increases from small values.^{2,4}

The influence of the plate spacing is shown in Fig. 5, where we present the highly asymmetric shapes of a short and tall bridge, and in Fig. 6 which reveals the effects of the plate spacing on the critical flow rate. For a given hysteresis $\theta_A - \theta_R$, increasing the plate separation from very small values, *increases* the critical flow rate Ca , for values of the plate separation up to $H/a = 1.101$ or $H/R = 1$, where R is the radius of a cylinder of the same volume. Above this value, increasing the plate separation *decreases* the critical flow rate.

This behavior is readily explained by the balance between the hydrodynamic and interfacial forces for different plate spacings. For very short bridges with advancing angles $\theta_A = 90^\circ$ and for very small deformations (i.e., for $\theta_A - \theta_R \rightarrow 0$), using the theory of the Hele-Shaw cell we may show that the hydrodynamic force is inversely proportional to the bridge height and scales as $\mu G a^3 H^{-1}$. By contrast, for very tall bridges, using slender-body theory we may show that the hydrodynamic force increases with the height of the bridge and scales as $\mu G H^2$. For both cases the interfacial force is proportional to the width of the contact line and hence decreases with the height of the bridge (for a given volume), yielding an overall scaling $\gamma(\theta_A - \theta_R) a^{3/2} H^{-1/2}$. Therefore, the capillary number Ca for short bridges scales as

$$(Ca)_{\text{short}} \sim (\theta_A - \theta_R)(H/a)^{1/2}, \quad (1)$$

while for tall bridges it scales as

$$(Ca)_{\text{tall}} \sim (\theta_A - \theta_R)(H/a)^{-5/2}. \quad (2)$$

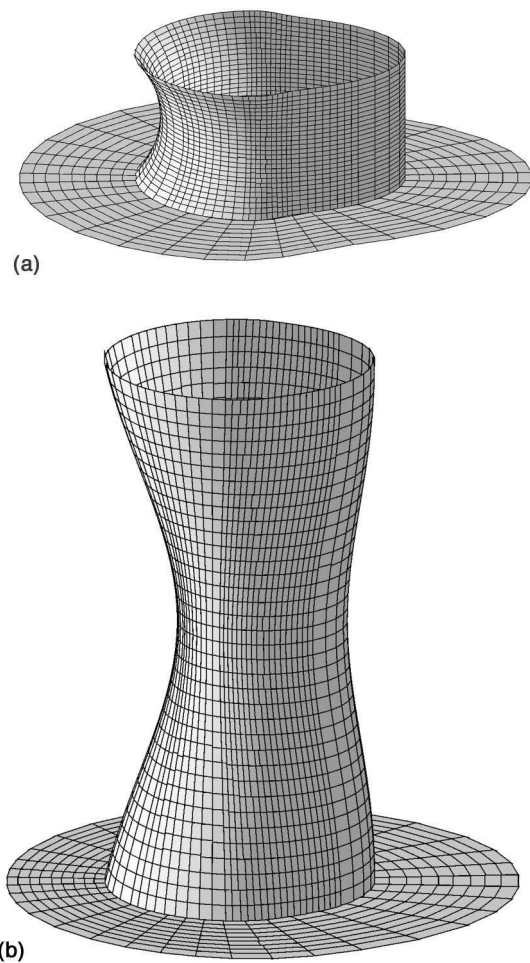


FIG. 5. Bridge surface with $\lambda=1$ and $\theta_A=90^\circ$ for different plate separations: (a) $H/a=1.101$ (or $H/R=1$) and $Ca=0.145$, (b) $H/a=3.218$ (or $H/R=5$) and $Ca=0.03$ (where R is the radius of a cylinder of the same volume).

This means that for a given hysteresis $\theta_A - \theta_R$ the critical capillary number Ca increases either when the plate separation increases from very small values or when the plate separation decreases from very high values. Thus there must be a value of the plate separation where the capillary number Ca takes a maximum value, as our computational results show. This behavior shows that very short or very tall bridges can be displaced more easily than bridges with moderate height. We note that this result is valid for any viscosity ratio, and thus it contrasts with the drop displacement results where a weak dependence on the plate spacing was found for viscous droplets, while a fast monotonic increase on the critical flow rate Ca was found for low-viscosity droplets (see Figs. 7, 9, and 13 in Ref. 4).

As a final point one may address the following question: for a specific parallel plate apparatus and a specific drop volume, what is more stable, a droplet attached to one plate or a fluid bridge between the two plates? The answer depends on the dimensionless plate spacing and the contact

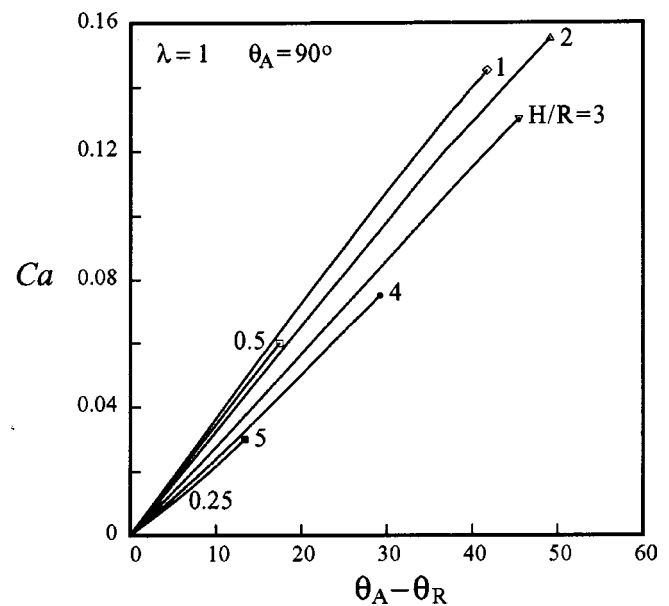


FIG. 6. Critical Ca vs hysteresis $\theta_A - \theta_R$ for a bridge with $\lambda=1$, $\theta_A=90^\circ$ and for different plate separations. (The curve for $H/R=0.25$ falls between the curves $H/R=2$ and 3 ; R is the radius of a cylinder of the same volume.)

angles. For very large plate spacings, even the quiescent bridge is unstable; thus in this case only the first configuration is stable. For other plate spacings, a qualitative answer can be given easily for bridges with moderate to large contact angles. For very small plate spacing, no solution exists for a single droplet; in this case only the bridge is a possible configuration. For moderate values of the plate separation, the viscous bridge is more stable since it forms two contact lines (i.e., they provide higher net interfacial forces), as can be easily verified by comparing our current results with our results for drop displacement in pressure-driven flows.⁴

ACKNOWLEDGMENTS

This work was supported by the National Science Foundation and the Petroleum Research Fund administered by the American Chemical Society. The computations were performed on multiprocessor computers provided by the National Center for Supercomputing Applications (NCSA) in Illinois.

¹E. B. Dussan V., "On the ability of drops to stick to surfaces of solids. Part 3. The influences of the motion of the surrounding fluid on dislodging drops," *J. Fluid Mech.* **174**, 381 (1987).

²P. Dimitrakopoulos and J. J. L. Higdon, "On the displacement of three-dimensional fluid droplets from solid surfaces in low-Reynolds-number shear flows," *J. Fluid Mech.* **377**, 189 (1998).

³P. Dimitrakopoulos and J. J. L. Higdon, "On the gravitational displacement of three-dimensional fluid droplets from inclined solid surfaces," *J. Fluid Mech.* **395**, 181 (1999).

⁴P. Dimitrakopoulos and J. J. L. Higdon, "On the displacement of three-dimensional fluid droplets adhering to a plane wall in viscous pressure-driven flows," *J. Fluid Mech.* **435**, 327 (2001).

⁵R. D. Gillette and D. C. Dyson, "Stability of fluid interfaces of revolution between equal solid circular plates," *Chem. Eng. J.* **2**, 44 (1971).